Research Article

Tao Song, Chao Liu, Hengxuan Zhu, Min Zeng, and Jin Wang*

A Novel Evaluation Method For Particle Deposition Measurement

https://doi.org/10.1515/phys-2019-0097
Received Sep 21, 2019; accepted Dec 16, 2019

Abstract: Normal operation of gas turbines will be affected by deposition on turbine blades from particles mixed in fuels. This research shows that it is difficult to monitor the mass of the particles deposition on the wall surface in real time. With development of electronic technology, the antenna made of printed circuit board (PCB) has been widely used in many industrial fields. Microstrip antenna is first proposed for monitoring particles deposition to analyse the deposition law of the particles accumulated on the wall. The simulation software Computer Simulation Technology Microwave Studio (CST MWS) 2015 is used to conduct the optimization design of the PCB substrate antenna. It is found that the S_{11} of vivaldi antenna with arc gradient groove exhibits a monotonous increase with the increase of dielectric layer thickness, and this antenna is highly sensitive to the dielectric layer thickness. Moreover, a cold-state test is carried out by using atomized wax to simulate the deposition of pollutants. A relationship as a four number of times function is found between the capacitance and the deposited mass. These results provide an important reference for the mass detection of the particle deposition on the wall, and this method is suitable for other related engineering fields.

Keywords: Gas turbine, deposition, microstrip antenna, return loss, vivaldi antenna.

PACS: 81.15.Fg, 84.40.Ba

***Corresponding Author: Jin Wang:** School of Energy and Environmental Engineering, Hebei University of Technology, Tianjin 300401, China; Key Laboratory of Thermo-Fluid Science and Engineering (Xi'an Jiaotong University), Ministry of Education, Xi'an 710049, China; Email: wjwcn00@163.com
Tao Song: School of Electronic and Information Engineering, Hebei University of Technology, Tianjin 300401, China
Chao Liu, Hengxuan Zhu: School of Energy and Environmental Engineering, Hebei University of Technology, Tianjin 300401, China
Min Zeng: Key Laboratory of Thermo-Fluid Science and Engineering (Xi'an Jiaotong University), Ministry of Education, Xi'an 710049, China

Nomenclature

τ time, [μs]
$\boldsymbol{C}$ Capacitance, [pF]
$\boldsymbol{P}_{inc}$ Incident power, [mW]
$\boldsymbol{P}_r$ Reflected power, [mW]
$\boldsymbol{R}$ Resistor, [Ω]
$\boldsymbol{U}$ Voltage, [V]
$\boldsymbol{U}_\tau$ Discharge threshold voltage, [V]
$\boldsymbol{U}_{th}$ Charge threshold voltage, [V]

1 Introduction

Gas turbine is a typical high-tech intensive product that represents one of the best technologies in the equipment manufacturing industry. As an advanced power machine, it was first widely applied in the aerospace and rapidly developed into other important fields (like power generation). Turbine inlet temperature increases with the requirement of the high thermal efficiency. For aviation industry, thermal protection is one of the key issues in developing high performance engines, especially in a scramjet [1]. Under high temperature environments, the interior insulator in the engine is pyrolyzed and charred so that it can no longer resist the mechanical damages caused by gas flow and particle erosion. Liu *et al.* [2] established a porous media volumetric ablation model to analyze this complex physicochemical process in porous structure of char layer. They pointed out that the local temperature had great influence on the pyrolysis gas deposition reaction in the char layer of ethylene-propylene-diene monomer (EPDM) insulation materials. It is very important to use efficient cooling technology to ensure the safe operation of the gas turbine. Film cooling shows that low-temperature air is injected from the discrete holes drilled on the surface of the turbine blade, and a cooling gas film is formed over the turbine blade to avoid the high-temperature gas directly impacting on the blade wall [3]. Ambient air contains some solid microparticles, which is provided to gas turbines during operation. Moreover, due to the rising cost of natural gas, synthetic gas extracted from fossil fuels has also been used as fuel

Open Access. © 2019 T. Song *et al.*, published by De Gruyter. This work is licensed under the Creative Commons Attribution 4.0 License

for land-based gas turbines [4]. Bons *et al.* [5] pointed out that more than two tons of impurities were ingested into a gas turbine during its 8,000 hours of operation. The particles contained in the air and the pollutants generated by the combustion of the fuel are softened and melted due to the high-temperature environment. When these molten particles impinge on the relatively cold wall of the blade, those particles will adhere to the vicinity of the film holes and produce more deposition on the surface of the turbine blade. Due to the particles deposition, the roughness of the turbine blade surface increases, and the aerodynamic performance becomes significantly worse [6]. The film holes may be blocked, which results in the deterioration of the cooling performance [7].

With development of computational fluid dynamics, the critical viscosity model [8] and the critical velocity model [9] were widely applied to reveal the mechanism of the particle deposition. Wang *et al.* [10] investigated the two models in their review paper. They pointed out that the predicted range of the critical viscosity model was limited by both temperature and velocities of particles, when these particles impacted on the walls. However, the critical velocity model cannot predict the viscosity at the critical temperature. Therefore, it is necessary to further develop or modify these two models. In the experimental aspect, Jensen *et al.* [11] developed a high-temperature turbine accelerated deposition facility (TADF) in which particles (mainly some impurities such as coal ash) were injected into the gas channel for the simulations of the long-term particle deposition. 10,000 hours of real turbine operation was simulated using TADF in a four-hour test. Using scanning electron microscope and x-ray spectroscopy, they found that the microstructure and chemical composition of the deposits were similar to those found on actual turbine blades. Crosby *et al.* [12] analyzed effects of particle size, gas temperature and wall temperature on deposition through the TADF platform. The results showed that the capture efficiency was improved when the particle size increases. Based on the TADF platform, Lewis *et al.* [13] obtained three deposition shapes using optical scanning equipment to replicate the real appearance of deposits, and they found that deposition upstream the cooling hole was beneficial for the improvement of the film cooling effectiveness. Considering that the experimental research using the molten coal ash in high-temperature environment has a high cost, Lawson *et al.* [14] used molten wax to simulate the particle deposition in a low-velocity wind tunnel. It was found that lower momentum flux ratio resulted in more deterioration of the cooling performance due to the presence of the deposition. In addition, they applied this method to a large scale turbine cascade to analyze the deposition process of the particles on the endwall [15]. It was found that most of the particles were clustered near the stagnation point downstream the leading edge. Albert *et al.* [16] improved the experimental device in Refs. [15, 16]. They studied the effect of the surface temperature of the blades model on the formation of the deposition.

Deposition of impurities in turbine engines is an extremely complicated physical process involving multiphase flow, *i.e.*, solid particles and molten particles (which are mixed with high-temperature gas). The existing numerical simulation model cannot accurately predict the deposition of the particles. In addition, coal ash under high temperature environment is melted in the TADF experimental device, which results in an increase in the research costs. As a low temperature phase change material, it has been proved that the paraffin can be used to simulate particle deposition. In order to obtain the mass of the particle deposition on the wall, the previously unhandy method is to scrape the deposition off the wall and then to use a balance scale to weigh its mass. However, this method cannot detect the quality of particle deposition in real time, and it also has big measurement errors. Therefore, it is needed to find some new method for the deposition measurement.

With the rapid development of modern electronic technology, microstrip antenna has been widely used in many industrial fields. Microstrip antenna is made of metal path, which has the advantages of small size, light weight and simple manufacturing process. In the actual measurement, it can be directly by attached to the wall surface for use. Gammoudi *et al.* [17] used the conductivity change based on Carbon Nanotube - Radio Frequency Identification (CNT-RFID) tag antennas to detect harmful gases. Their results showed that the proposed antenna exhibited good performance due to the impedance variation of the tag antenna caused by harmful gases. Liu *et al.* [18] designed a single-piece capacitance sensor to measure the thickness of thin film from nm-level to micron-level. Yin and Horoshenkov [19] estimated the thickness of the deposition on the bottom of the rectangular pipe by comparing the frequency of the measured propagation mode. The frequency was calculated by the finite element method (FEM), and the feasibility of this method was validated with experiments. In aerospace, Khan [20] used a rectangular microstrip patch antenna to test the ice thickness changes in antenna impedance.

Operating life of turbo-machinery will be shortened due to presence of particle deposition. Previous studies have shown that the particle deposition on the wall is difficult to detect in real time. In this paper, atomized molten wax particles are used to simulate pollutants in gas turbine. Moreover, a new evaluation method for the particle deposition measurement is proposed. A microstrip antenna is used to detect the deposition of the particles on the wall. This research is mainly divided into two parts. In the first part, the full-wave simulation software based on finite element method is used to optimize the PCB measurement substrate. In the second part, according to the simulated antenna model, the PCB board is made for experimental tests, and the prediction of the deposition is discussed at final.

2 Experimental facility

Figure 1 shows the diagram of the experimental system which is mainly divided into three parts: compressed air supply section, liquid wax supply section, and testing section. Air supplied by the compressor is preheated by a heat exchanger. A container with solid wax is immersed in a water bath at constant temperature, and the wax is kept in a liquid state due to the heat from the hot water. The Polyvinyl chloride (PVC) pipes which connect different experimental sections are wrapped by thermal insulation materials. The liquid wax is sucked into the nozzle by the compressed air due to a negative pressure inside the nozzle. A siphon atomizing nozzle is used to generate tiny wax particles with a diameter of about 15 µm. The flow rate of the molten wax sprayed from the nozzle is 0.52 g/s. Moreover, a grid configuration is arranged at the exit of the test section, and a small bag filter is installed behind the grid to recycle the wax.

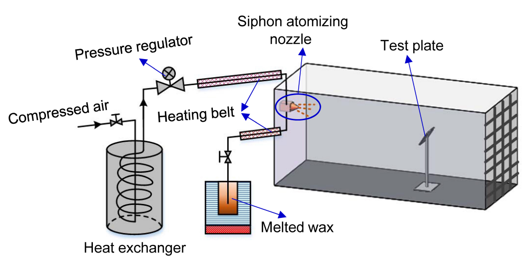

(a) Schematic diagram of experimental system

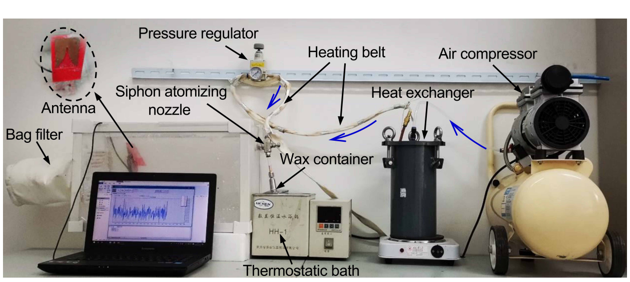

(b) Actual experimental devise

Figure 1: Experimental system

The experimental section is a rectangular box with dimensions of 500×200×300 mm, and this box is made of transparent acrylic plate. The distance l between the support frame and the inlet is 300 mm, and the height of the support frame (h_2) is 150 mm. The mounting height of the atomizing nozzle (h_1) is 180 mm. In addition, the atomizing nozzle and the support frame are located in the middle of the test section. The antenna is fixed on the flat plate of the support frame to detect the quality of the paraffin particle deposition, and the angle of the antenna in the vertical direction (α) is 30°.

The molten wax is used to simulate the deposition of the molten pollutants within the engine. In the tests, the used paraffin wax 58 has a solidification temperature of 58°C and a density of 900 kg/m^3. The mass of the wax deposition is measured by electronic balance, and the accuracy of the electronic balance was 0.0001 g. The stability of the compressed air is maintained by adjusting the pressure regulating valve. The pressure is constant at 0.8 MPa.

3 Measuring principle

An antenna structure is designed to detect the amount of atomized paraffin particles deposited on the wall. The feeder of the microstrip antenna and the ground can be simplified with two electrode plates of the capacitor. When the particles are deposited on the surface of the microstrip antenna, the dielectric constant of the microstrip antenna increases due to a reduction of the capacitance. With decreasing the capacitance, the resonant frequency point of the microstrip antenna also increases, which causes the shift of the frequency point of the microstrip antenna (S_{11}). The simulation software CST MWS 2015 is used to carry out variable scanning of antenna size and dielectric layer thickness to find a suitable antenna shape, and the S_{11} value is sensitive to the thickness variation of the dielectric layer. However, the microstrip antenna is considered as a capac-

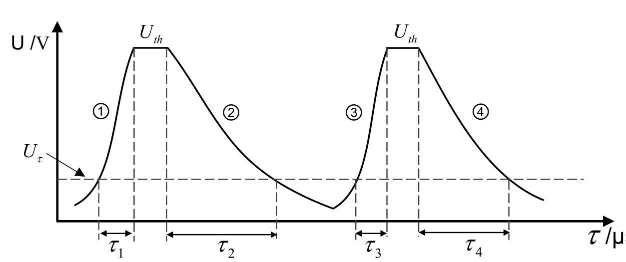

Figure 2: Charging and discharging processes

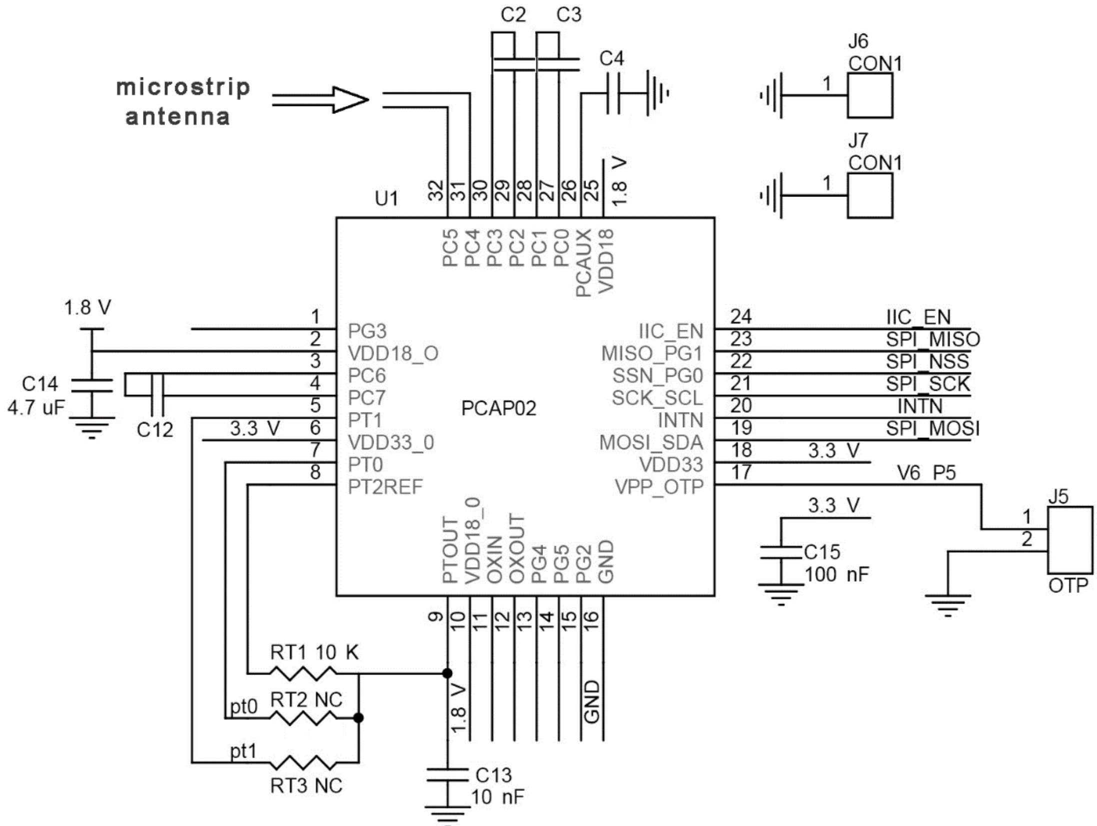

Figure 3: Circuit diagram of capacitor module

itor, and a known reference capacitor is used as a sample. The capacitance of the detecting antenna is calculated based on a comparison of charging time and discharging time of the two capacitors. Especially, RC charge and discharge circuits are applied for present measurements. Figure 2 shows the workflow:

1. In the part 1 of the process, the reference capacitor is charged to a high level U_{th}, and τ_1 is the charging time.
2. In the part 2 of the process, the reference capacitor is discharged to a low level, and τ_2 is the discharging time.
3. In the part 3 of the process, the microstrip antenna is charged as a capacitor, and τ_3 means the time of the second charging to the voltage U_{th}.
4. In the part 4 of the process, the microstrip antenna is discharged as a capacitor, and τ_4 means the time of the second discharging to the same low voltage as in step 2.

The measuring process is divided into two parts: charging and discharging stages. In this research, the discharging stage is analyzed by using the following equations:

$$U_\tau = U_{th} * \exp\left(-\tau/RC\right) \tag{1}$$

$$U_\tau = U_{th} * \exp(-\tau_2/RC_r) = U_{th} * \exp(-\tau_4/RC_m) \tag{2}$$

$$\tau_2/RC_r = \tau_4/RC_m \tag{3}$$

$$\tau_2/\tau_4 = C_r/C_m \tag{4}$$

When the microstrip antenna discharging time τ_4 is monitored, the corresponding capacitance can be obtained. The PCAP02 chip made by AMS sensor company, and its peripheral circuits are used as a measurement unit. Serial Peripheral Interface (SPI) protocol for communication with the microcontroller is used for the chip PCAP02, and the circuit is shown in Figure 3.

4 Results and discussion

In this paper, paraffin was used to simulate the deposition of particles. Influence of microstrip antenna structure on particle deposition detection was analyzed.

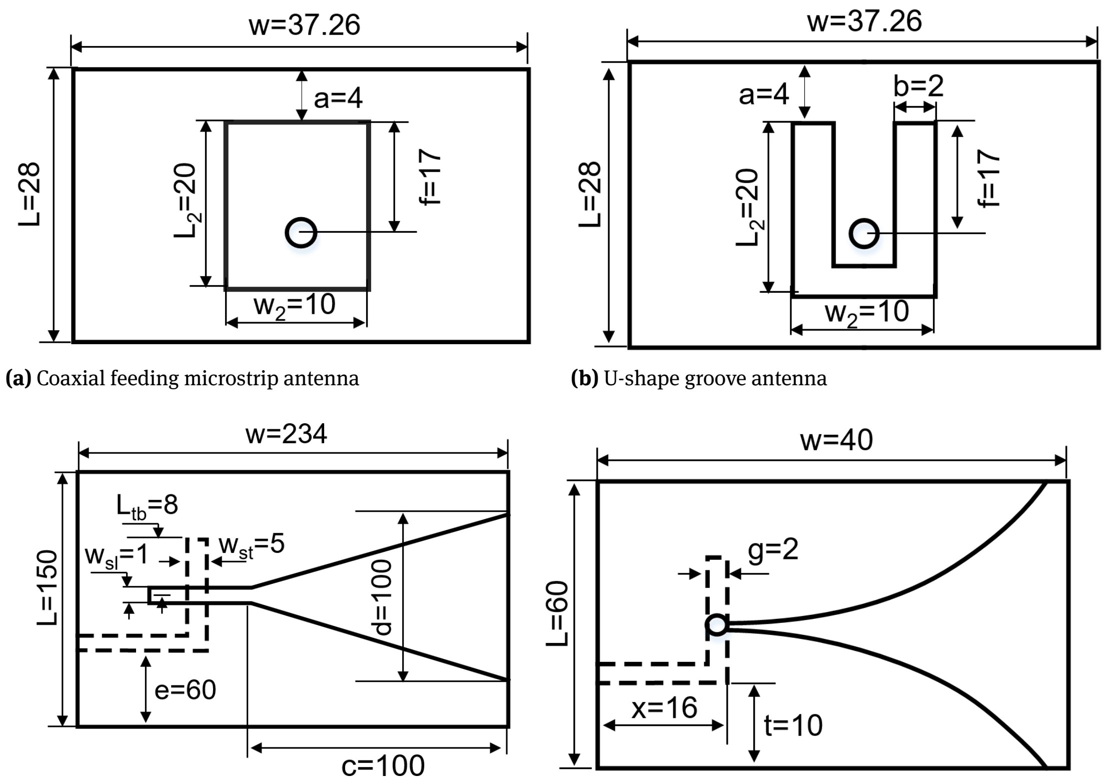

(a) Coaxial feeding microstrip antenna

(b) U-shape groove antenna

(c) Linear gradient gap antenna

(d) Vivaldi antenna

Figure 4: Four microstrip antenna configurations and detailed parameters (unit: mm)

4.1 Comparison of various antennas

In order to find a suitable size and high sensitivity microstrip antenna, the antenna configuration is optimized using simulation software CST MWS. Four microstrip antennas are selected from Refs. [21–24], *i.e.*, coaxial feeding microstrip antenna, U-shape groove antenna, linear gradient gap antenna and vivaldi antenna. The detailed dimensions and parameters of these antennas are presented in Figure 4. The dielectric constant of the deposition layer is set to 2.0.

S_{11} represents the return loss characteristic. Return loss (RL) is a parameter that represents the performance of the incident power reflected back to the signal source, and it is defined as the ratio of the incident power to the reflected power. The numerical relationship between RL and S_{11} is given by the following formula:

$$RL = \frac{P_{inc}}{P_r} \tag{5}$$

$$S_{11} = -RL \tag{6}$$

Figure 5 shows the S_{11} variation of various antennas with different dielectric layer thickness. The S_{11} of coaxial feeding microstrip antenna is not sensitive to the increase of dielectric layer thickness, *i.e.*, a small variation range of S_{11} from −28 dB to −31 dB. A phenomenon of rewinding is observed when the thickness of the dielectric layer is over 1.5 mm. This is because the design of the coaxial feeder microstrip antenna original has a narrow operating bandwidth. U-shape groove and linear gradient gap antennas show irregular trends. Moreover, as the thickness of the dielectric layer increases, the S_{11} fluctuation range of these two antennas changes little, which is mainly caused by the antenna construction. Especially, the u-shaped groove antenna has multiple operating frequency characteristics. The linear gradient gap antenna has a non-connection point when the slot surface changes from a rectangular shape to a linear gradient shape. Therefore, the three antennas mentioned above are not suitable for particle deposition testing. Compared to the other antennas, vivaldi antenna shows a significant monotonous growth trend of the S_{11} is obtained with the increases in the dielectric layer thickness.

Figure 6 shows the relationship between S_{11} and the dielectric thickness of the antenna. It can be seen that with the increase in the dielectric thickness, the S_{11} for both

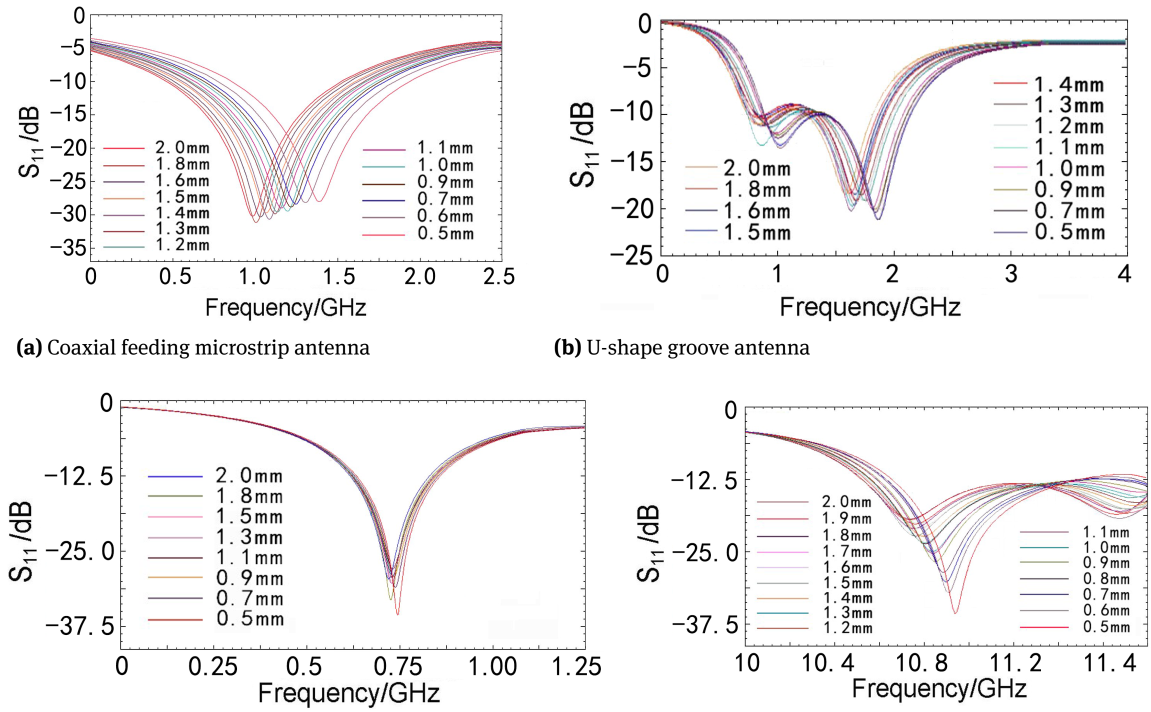

(a) Coaxial feeding microstrip antenna **(b)** U-shape groove antenna

(c) Linear gradient gap antenna **(d)** Vivaldi antenna

Figure 5: S_{11} varies with the thickness of the dielectric layer

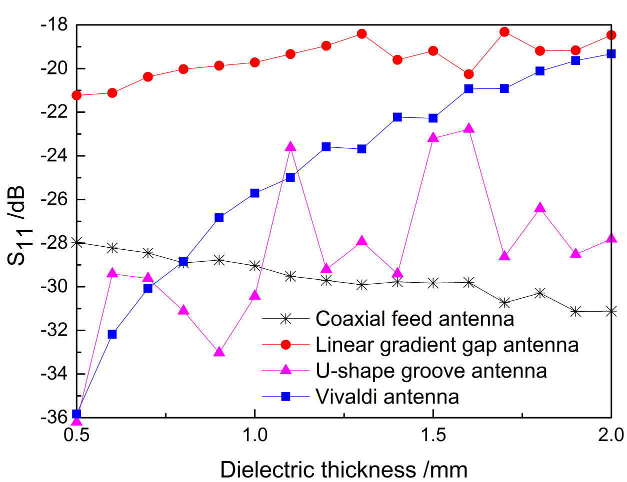

Figure 6: Relation between dielectric thickness and S_{11} of microstrip antenna

the coaxial feed antenna and linear gradient gap antenna show a relatively even trend compared to other antennas. This result indicates that the coaxial feed and linear gradient gap antennas are not sensitive enough as detection sensors. Based on the effect of the dielectric thickness, the S_{11} variation of the U-slot antenna is very chaotic. It is concluded that these three antennas cannot be used as sensors for the deposition measurement. The vivaldi antennas can meet the requirement of the deposition measurement due to the both good sensitivity and variation regularity to the dielectric thickness.

4.2 Experimental results

According to the comparison of various antennas, the most suitable antenna model is the microstrip antenna structure with curved gradient. A PCB-level antenna sample is fabricated, and the antenna structure is connected to the capacitive sensor for practical tests. To reduce the human error, the antenna is fixed on the support frame in the test section. The molten paraffin is sucked into the siphon nozzle under the negative pressure, and the fine particles of the paraffin are ejected out of the nozzle outlet. Figure 7 shows deposition images using wax particles with time. It can be seen that the wax particles are deposited uniformly on the surface of the antenna, and there is a certain space between the particles. It is difficult to accurately measure the thickness of the wax particles deposited on the surface during the real process. The deposited mass is chosen as a suitable measurement parameter for this research. It is found that the mass of the particles deposited on the antenna surface gradually increases with time, which affects

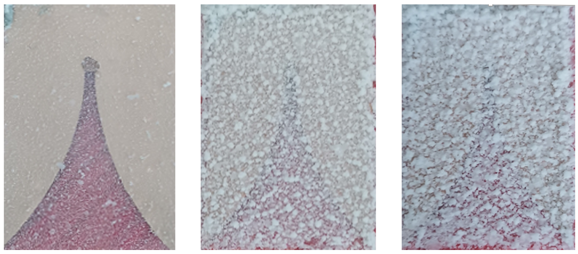

(a) 20 s, 0.13 g **(b)** 75 s, 0.51 g **(c)** 135 s, 0.86 g

Figure 7: Images of deposition using wax particles with time

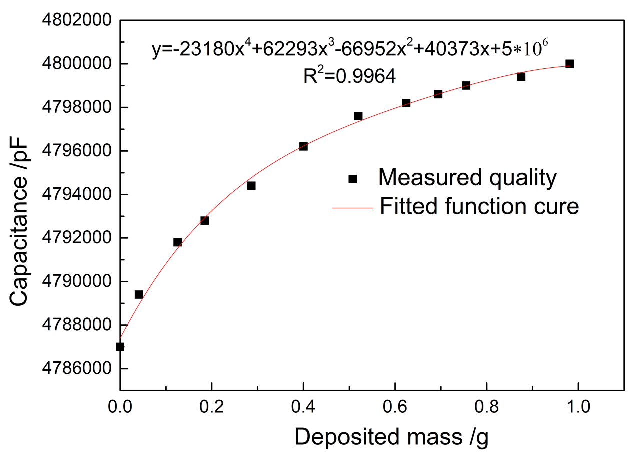

Figure 8: Relationship between the capacitance and the deposited mass of wax particles

the capacitance value detected by the capacitance sensor.

Figure 8 shows the relationship between the measured antenna capacitance and the deposited mass of wax particles. It can be seen that the capacitance value increases as the deposited mass increases. When the deposited mass is between 0 and 0.6 g, the capacitance is very sensitive to the deposition of the wax particles, and the capacitance fluctuation shows a large range. However, with a deposition range between 0.6 and 1.0 g, the capacitance increases slowly and gradually approaches an equilibrium value. This is mainly because the antenna capacitance will be insensitive to the increase in wax deposition, when the wax particle deposition reaches a certain thickness on the surface of the antenna. Finally, a function curve is fitted based on the measured quality of the wax deposited as follows:

$$y = 23180x^2 + 62293x^3 - 66952x^2 + 40373x + 5 \times 10^6 \quad (7)$$

5 Conclusions

In this paper, a novel method is proposed to detect particle deposition in real time based on a capacitive effectiveness of microstrip antennas. Influence of four microstrip antennas S_{11} on the thickness of the dielectric layer was discussed by using CST MWS 2015. During the tests, a PCB substrate antenna with arc gradient groove was designed, and atomized wax particles were used to simulate the deposition of pollutant particles.

Compared to the traditional weighing method, this new method can detect the deposition in real time. Numerical results show that the S_{11} of the coaxial feeding antenna is not sensitive to the increase of the thickness of the dielectric layer. As the thickness of the dielectric layer increases, both the U-shape groove antenna and the linear gradient gap antenna S_{11} show an irregular trend. The S_{11} of the vivaldi antenna shows a regular increase with increasing the dielectric layer thickness. In addition, the feasibility of the vivaldi antenna is further proved by present experimental tests. Based on measured data, it is concluded a quadratic function relationship between the vivaldi antenna capacitance and the deposited mass. The deposition mass can be calculated by the changeable value of the antenna capacitance. This provides the possibility for the remote monitoring and real-time detection of the particle deposition. At the same time, this research provides an important reference for other engineering applications involved with detection of particle deposition.

Acknowledgement: This work is supported by the National Natural Science Foundation of China [Grant No. 51606059], the Key research project of Hebei province (No. 19227212D) and the Foundation of Key Laboratory of Thermo-Fluid Science and Engineering (Xi'an Jiaotong University), Ministry of Education, Xi'an 710049, P.R. China (Grant No. KLTFSE2018KFJJ01).

References

[1] Jiang Y.G., Feng Y., Zhang S.L., Qin J., Bao W., Numerical heat transfer analysis of transcritical hydrocarbon fuel flow in a tube partially filled with porous media, Open Phys., 2016, 14, 659-667.

[2] Liu Y., Jing Y.X., Ming M.J., Guan Y.W., Li J., Li Q., et al., A volumetric ablation model of EPDM considering complex physicochemical process in porous structure of char layer, Open Phys., 2017, 15, 344-353.

[3] Han J., Fundamental gas turbine heat transfer, J. Therm. Sci. Eng. Appl., 2013, 5, 021007.

[4] Lewis S., Barker B., Bons J.P., Ai W., Fletcher T.H., Film cooling effectiveness and heat transfer near deposit-laden film holes, J. Turbomach., 2011, 133, 031003.

[5] Pons J.B., Crosby J., Wammack J.E., Bentley B.I., Fletcher T.H., High-pressure turbine deposition in land-based gas turbines from various synfuels, J. Eng. Gas Turbines Power, 2015, 129, 135-143.

[6] Abuaf N., Bunker R.S., Lee C.P., Effects of surface roughness on heat transfer and aerodynamic performance of turbine airfoils, J. Turbomach., 1998, 120, 522-529.

[7] Kim J., Dunn M.G., Baran A.J., Wade D.P., Tremba E L., Deposition of volcanic materials in the hot sections of two gas turbine engines, J. Eng. Gas Turbines Power, 1993, 115, 641-651.

[8] Sreedharan S.S., Tafti D.K., Composition dependent model for the prediction of syngas ash deposition in turbine gas hotpath, Int. J. Heat Fluid Fl., 2011, 32, 201-211.

[9] Ai W., Fletcher T.H., Computational analysis of conjugate heat transfer and particulate deposition on a high pressure turbine vane, J. Turbomach., 2011, 134, 041020.

[10] Wang J., Vujanovic M., Sunden B., A review of multiphase flow and deposition effects in film-cooled gas turbines, Therm. Sci., 2018, 22, 1905-1921.

[11] Jensen J.W., Squire S.W., Bons J.P., Fletcher T.H., Simulated land-based turbine deposits generated in an accelerated deposition facility, J. Turbomach., 2004, 127, 462-470.

[12] Crosby J.M., Lewis S., Bons J.P., Ai W., Fletcher T.H., Effects of temperature and particle size on deposition in land based turbines, J. Eng. Gas Turbines Power, 2008, 130, 051503.

[13] Lewis S., Barker B., Bons J.P., Ai W., Fletcher T.H., Film cooling effectiveness and heat transfer near deposit-laden film holes, J. Turbomach., 2011, 133, 031003.

[14] Lawson S.A., Thole K.A., Effects of simulated particle deposition on film cooling, J. Turbomach, 2011, 133, 021009.

[15] Lawson S.A., Thole K.A., Simulations of multiphase particle deposition on endwall film-cooling, J. Turbomach., 2012, 134, 011003.

[16] Albert J.E., Bogard D.G., Experimental simulation of contaminant deposition on a film-cooled turbine vane pressure side with a trench, J. Turbomach., 2013, 135, 051008.

[17] Gammoudi I., Nedil M., Aissa B., Gas sensor based on RFID tag antenna for harsh environment, International Symposium on Antennas and Propagation, Fajardo, Puerto Rico, 2016, 1271-1272.

[18] Liu C., Chen Y., Guo X., Zhang Y., Measure thickness of magnetic thin-film based on the capacitance-to-frequency signal conversion, International Conference on Internet Computing and Information Services, Hong Kong, China, 2011, 378-380.

[19] Yin Y., Horoshenkov K.V., Determination of thickness of the sediments in a rectangular pipe by modal frequencies' shift, International Conference on Environmental Science and Information Application Technology, Wuhan, China, 2009, 597-600.

[20] Khan S.M., The design of a single frequency ice gauge using a microstrip patch antenna, International Symposium on High Performance Electron Devices for Microwave and Optoelectronic Applications, Glasgow, UK, 2000, 140-145.

[21] Chakraborty S., Mukherjee U., Comparative study of micro strip patch line feed and coaxial feed antenna design using genetic algorihms, International Conference on Computer and Communication Technology, Allahabad, India, 2011, 26-31.

[22] Bhan C., Dwivedi A.K., Mishra B., Kumar A., Quad Bands U-Shaped Slot Loaded Probe Fed Microstrip Patch Antenna, International Conference on Advances in Computing and Communication Engineering, Dehradun, India, 2015,409-412.

[23] Chen Q., Zhang H., Zhang X., Jin M., Wang W., Wideband RCS reduction of vivaldi antenna using electromagnetic band gap absorbing structure, International Symposium on Antennas and Propagation, Phuket, Thailand, 2017, 1-2.

[24] Herzi R., Bouslama M., Osman L., Gharsallah A., Frequency agile Vivaldi antenna with enhanced gain for wireless applications, International Microwave Workshop Series on Advanced Materials and Processes for RF and THz Applications, Pavia, Italy, 1-3.